Rotating RF Coil (RRFC) for flip angle and specific absorption rate management applications at 7T MRI

Adnan Trakic[1], Jin Jin[1], Mingyan Li[1], Darryl McClymont[1], Ewald Weber[1], Hector Sanchez Lopez[1], Miguel Fuentes[1], Feng Liu[1], and Stuart Crozier[1]
[1]*The School of Information Technology and Electrical Engineering, The University of Queensland, Brisbane, QLD, Australia*

Introduction: Recently, the single-channel mechanically Rotating RF Coil (RRFC) concept [1] was introduced as a complementary modality to Parallel Coil Arrays (PCAs). This numerical study explores the feasibility of using the RRFC for flip angle (FA) and specific absorption rate (SAR) management applications at high-field MRI. This new approach was compared against an 8-channel head PCA (8-PCA) under identical model settings at 7T. Since there is only one RF source operating at any given time, the (serial) RRFC excitation approach does not produce constructive and destructive wave interference, and since there is also a larger number of effective magnetic field profiles available at the end of the excitation, the RRFC produced a more uniform FA and a lower SAR compared to the PCA.

Method: Fig.1 (a) shows the RRFC and 8-PCA cylindrical setups (diameter = 288 mm, length = 260 mm, all coil loops had 30^o loop opening) and the 4mm-resolution Brooks Airforce head model, wherein the dielectric properties of the 24 tissue types frequency scaled to 298 MHz. A previously validated finite-difference time-domain (FDTD) method [2-3] was used to simulate the EM field propagation through the inhomogeneous head. In the RFFC case, a total of 120 simulations were performed individually with the RF coil displaced by a constant angle of $\Delta\theta = 3^o$, to effectively emulate the motion of the RF coil. Unit currents were applied to both the RRFC (for every position $\theta = q\Delta\theta$) and the 8-PCA (for each coil). All results were thereafter scaled equally and linearly so that the whole-body average FA was 30^o. For the two setups, the FA and SAR were calculated as follows [4]: $\mathrm{FA}_{paral.}(\mathbf{r}) = \gamma\mu_0 \left|\sum_{q=1}^{Q_p}\sum_{n=1}^{N} \mathrm{b}_n(\mathrm{q})\mathrm{H}_{1,n}^{+}(\mathbf{r})\right|$; $\mathrm{FA}_{serial}(\mathbf{r}) = \gamma\mu_0 \left|\sum_{q=1}^{Q_s} \mathrm{b}(\mathrm{q})\mathrm{H}_{1}^{+}(\mathbf{r},\mathrm{q})\right|$; $\mathrm{SAR}_{\mathrm{VOX}}^{\,paral.}(\mathbf{r}) = \frac{1}{T}\int_t^{t+T} \frac{\sigma(\mathbf{r})}{2\rho(\mathbf{r})} \left|\sum_{n=1}^{N} \mathrm{b}_n(\mathrm{t})\mathbf{E}_n(\mathbf{r})\right|^2 dt'$; $\mathrm{SAR}_{\mathrm{VOX}}^{\,serial}(\mathbf{r}) = \frac{1}{T}\int_t^{t+T} \frac{\sigma(\mathbf{r})}{2\rho(\mathbf{r})} \sum_{q=1}^{Q_s} \left|\mathrm{b}_q(\mathrm{t})\mathbf{E}_q(\mathbf{r})\right|^2 dt'$ and in both cases $\mathrm{SAR}_{10\mathrm{g}}(\mathbf{r}) = \int_{\mathbf{r}'\in \mathrm{V}_{10g},\mathbf{r}} \mathrm{SAR}_{\mathrm{VOX}}(\mathbf{r})\, d\mathbf{r}'$ where γ is the gyromagnetic ratio, μ_0 is the permeability of free space, q is index in time, Q_p and Q_s are the total number of RF pulse samples for PCA and RRFC, respectively, n denotes the n^{th} coil in the array of N coils, $\mathbf{r}$ is the position vector for a single voxel, $\mathrm{b(t)}$ denotes the complex RF pulse waveform, $\mathrm{H}_1^+(\mathbf{r})$ is the spatial RF transmit profile of the magnetic field intensity, i denotes the complex number, $\mathbf{E}(\mathbf{r})$ is the steady-state complex electric field vector, $\sigma(\mathbf{r})$ is the electrical conductivity, $\rho(\mathbf{r})$ is the mass density of the sample, t is the time parameter and T is the 6min period over which the SAR was time averaged according to [ref]. The 10g-averaged SAR (i.e. $\mathrm{SAR}_{10g}(\mathbf{r})$) was calculated over a voxel volume that best approximates 10g of tissue (in this case 5x5x5 voxels). For all simulations, the TR and the duration of the hard RF pulse (square wave) τ were set to 20 ms and 5 ms, respectively. It was assumed that RRFC makes one revolution during the time when the RF pulse is applied (i.e. T_{rot} = 5 ms; ω_{rot} = 1,256.6 rads^{-1}).

Results and Discussions: Fig.1 (b) compares the RRFC and the 8-PCA in terms of the four parameters: FA, E field, $\mathrm{SAR_{VOX}}$ and $\mathrm{SAR_{10g}}$. While 8-PCA produced the typical central brightening at 7 T and local SAR hotspots, the RRFC arrangement yielded a much more homogeneous FA distribution and lower values of SAR under same conditions. The table in Fig.1 (c) lists the average, standard deviation and maximum values of the four parameters, for both setups. While 8-PCA arrangement produced a maximum FA of 102.8^o (and FA standard deviation of 6.6^o), RRFC yielded a much smaller maximum FA of 58.1^o (with standard deviation of 4.6^o). Similarly, RRFC produced 23% lower $\mathrm{SAR_{VOX}}$ and 17% lower $\mathrm{SAR_{10g}}$ than 8-PCA. Fig.1 (d) is the corresponding box and whisker plot (in terms of FA and $\mathrm{SAR_{10g}}$) shows improved performance of RRFC, due to the fact that it had: (1) the narrowest lower-to-upper-quartile FA distribution centered on the target FA = 30^o and (2) the lowest maximum $\mathrm{SAR_{10g}}$. Based on the theory and supporting results, the progression of the EM fields and therefore, the corresponding FA and SAR distributions, differs for the parallel and serial (or time-multiplexed RRFC) excitation. With parallel excitation, the EM fields due to N simultaneously operating current sources produce constructive and destructive interferences, which result in FA non-uniformities and high local SAR. In contrast, with the serial excitation (i.e. RRFC), as only one EM source operates at a given time, there is no constructive and destructive interference of EM waves, and since there is also a larger number of effective magnetic field profiles available at the end of the excitation, the RRFC technique produces a more uniform magnetic field (and corresponding FA) and a lower local electric field (and corresponding SAR) distribution compared to PCA.

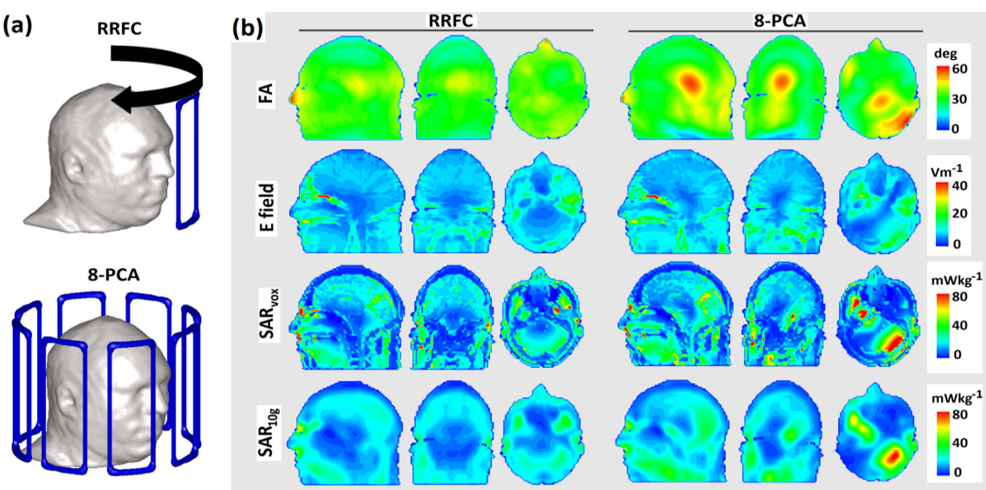

(c)

	RRFC			8-PCA		
	Avg.	Std.	Max.	Avg.	Std.	Max.
FA	30.0	4.6	**58.1**	30.0	6.6	**102.8**
|E|	9.9	4.3	**97.6**	9.5	4.9	**92.5**
SAR_{VOX}	17.4	15.8	**355.1**	17.6	19.6	**461.8**
SAR_{10g}	17.3	6.2	**70.2**	17.5	10.5	**83.6**

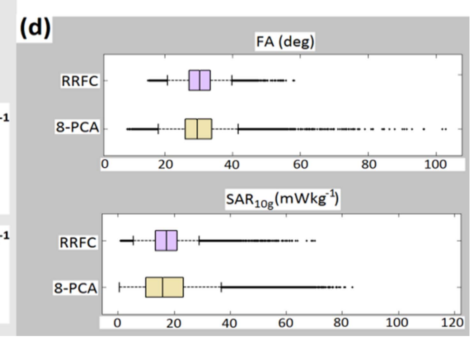

Fig.1 – Model setup: (a) the Rotating RF Coil (RRFC) and the 8-channel PCA. **Results: (b)** central coronal, sagittal and axial slices of the FA, E field, voxel SAR and 10g-averaged SAR for both RRFC and 8-PCA; **(c)** table listing average (Avg.), standard deviation (Std.) and maximum (Max.) values of the same parameters as in (b) for the entire head volume; and **(d)** corresponding box and whisker plot of the FA and $\mathrm{SAR_{10g}}$.

Conclusion: Compared to the 8-PCA, RRFC yielded a more uniform FA distribution and a lower $\mathrm{SAR_{VOX}}$ and $\mathrm{SAR_{10g}}$. This initial study suggests that RRFC may be useful in alleviating the FA/SAR issues associated with contemporary high field MRI. Additional experiments are underway.

References: [1] A. Trakic *et. al. J. Magn. Reson*. 201: 186-198, 2009; [2] Taflove, Computational Electrodyamics, Boston, MA: Artech, 1995; [3] F. Liu *et. al. Phys. Med. Biol*, 49: 1835-1851, 2004; [4] A. Trakic *et. al. J. Magn. Reson*, 236: 70-82, 2013.